On Improved Network Models for Rubber Elasticity and Their Applications to Orientation Hardening in Glassy Polymers

Wu, P.D.; Giessen, E. van der

Published in:
Journal of the Mechanics and Physics of Solids

DOI:
10.1016/0022-5096(93)90043-F

J. Mech. Phys. Solids Vol. 41, No. 3, pp. 427–456, 1993.
Printed in Great Britain.

0022–5096/93 $6.00 + 0.00

ON IMPROVED NETWORK MODELS FOR RUBBER ELASTICITY AND THEIR APPLICATIONS TO ORIENTATION HARDENING IN GLASSY POLYMERS

P. D. WU and E. VAN DER GIESSEN

Laboratory for Engineering Mechanics, Delft University of Technology, Delft, The Netherlands

(*Received* 10 *April* 1992; *in revised form* 12 *August* 1992)

ABSTRACT

THREE-DIMENSIONAL molecular network theories are studied which use a non-Gaussian statistical mechanics model for the large strain extension of molecules. Invoking an affine deformation assumption, the evolution of the network—consisting of a large number of molecular chains per unit volume, which are initially randomly oriented in space—is shown to be governed by a balance equation in orientation space. Eulerian and Lagrangian type formulations of these balance equations are given, and the closed-form analytical solution for the so-called Chain Orientation Distribution Function is derived. This full network model is then used to describe the large strain inelastic behaviour of rubber-like materials. Detailed comparisons with experimental results and with two approximate models, namely the classical three-chain model and a very recently proposed eight-chain model, are provided for different types of deformation and rubbers. Finally, the network model is applied to describe the orientational hardening in amorphous glassy polymers, and confronted with experimental data for polycarbonate. The inherent physical limitations of the network theory for both applications are discussed.

1. INTRODUCTION

THE CONSTITUTIVE DESCRIPTION of rubber elasticity by application of macromolecular network models dates back to as early as the 1940s. TRELOAR (1975) gives an excellent comprehensive treatment of the subject. These theories are based on the concept of a network of chains of randomly oriented rigid links that are connected at junction points which in rubber-like materials are provided by the chemical cross-links between macromolecules. The stiffness of such a network is associated with the changing configurational entropy of the network chains. The first statistical mechanics considerations of long chains assumed Gaussian statistics for the possible chain configurations, and it was found that the response of the entire network consisting of n randomly oriented chains per unit volume is identical to that of three independent sets of $n/3$ single chains in three orthogonal directions (see e.g. JAMES and GUTH, 1943). Non-Gaussian statistics were employed subsequently to single chain configurations (KUHN and GRÜN, 1942) taking into account the finite extensibility of molecular chains. However, the implementation of such a more accurate statistical theory for a single chain into a theory for the entire networks of chains is far more complex than in the Gaussian theory. For uniaxial extension, JAMES and GUTH (1943) suggested

developing an approximate network model based on the simplifying assumption that the property of the Gaussian network of being equivalent to three independent sets of chains may be taken over into the non-Gaussian theory (see also Wang and Guth, 1952). Thus, the actual spatial distribution of chains is sampled in three orthogonal orientations. Similarly, Treloar (1946) proposed the use of the idea of a four-chain Gaussian network representation (Flory and Rehner, 1943) to sample four spatial chain orientations. Somewhat later, Treloar (1954) formulated a full network theory for simple uniaxial extension which accounts for the actual spatial distribution of chain orientations, but this remained virtually dormant for about 25 years until Treloar and Riding (1979) extended the theory to biaxial tensile deformations along fixed axes and actually carried out the averaging procedure. Such a full network theory can only be handled numerically, however, and therefore the simplest three-chain model has become the most widespread and almost standard non-Gaussian network model.

Network theories have also found an application in the constitutive description of non-rubber-like materials, such as amorphous polymers below their glass transition temperature. When subjected to large strains, and after plastic flow has been initiated, such materials exhibit very strong strain hardening, which is primarily the result of straightening out of polymer chains between physical entanglements and the associated orientation of molecular chains. Haward and Thackray (1968) suggested for a one-dimensional model that this orientation hardening could be modelled by the application of a non-Gaussian chain theory. Recently, Boyce *et al.* (1988) extended this to a general three-dimensional model (which we shall term the BPA model) by adopting the three-chain network model. This model turned out to be able to predict some of the well-known phenomena during large strains of polymers rather well, but it was found very recently by Arruda and Boyce (1991) to be unable to capture the dependence of strain hardening on the state of deformation found experimentally in their large strain experiments on polycarbonate (PC). At the same time, they proposed to model the network by eight equivalent chains instead of three.

A detailed study of that eight-chain model for rubber elasticity in comparison with experiments on various kinds of rubber has appeared very recently (Arruda and Boyce, 1992a), and much better agreement with experiments was obtained than with the traditional three-chain model. A study of the orientation hardening in glassy polymers by the same authors has revealed similar trends (Arruda and Boyce, 1992b). Obviously, the three-chain and eight-chain models are but approximate representations of the actual spatial distribution of molecular chains. Among all possible orientations these models can be regarded to sample a set of particular directions. However the accuracy of these approximations has not been established.

The purpose of this paper is to assess the accuracy of the three- and eight-chain models by comparison with a model which accounts accurately for the actual spatial orientation distribution of molecular chains. Treloar and Riding (1979) have already developed a rubber elasticity theory based on such a full network description; but, their considerations were limited to deformations with biaxial extension along fixed axes under plane stress conditions. In the present paper we extend their work to a general formulation valid for three-dimensional deformation processes. In the first part, we focus attention on rubber networks deforming affinely with the continuum

deformation [a few preliminary results have been reported by WU and VAN DER GIESSEN (1992)], and in the second part we discuss the application of the network theory to describe the anisotropic strain hardening in amorphous polymers. The modelling centres around a general treatment of the orientation distribution of molecular chains and their evolution as deformation progresses. This description utilizes the idea of Chain Orientation Distribution Function (CODF), which is governed by balance equations that express physically well-understood conservation features. The authors are not aware of any comparable treatment for networks. Assuming the network to deform affinely with the deformation of the continuum in which it is embedded, closed-form solutions are derived for this CODF, which thus contain the complete information of the orientation distribution of molecular chains at any stage of the deformation. This solution is then used to develop the rubber elasticity model by averaging out the contribution to the free energy of individual chains over all chain orientations. In a modified form, similar to the work of BOYCE *et al.* (1988), this full network model is used to model orientation hardening in glassy polymers. The full network model requires numerical integration; an approximation based on the three- and eight-chain representations turns out to be very accurate over the entire range of strains. Verification with some experimental results from the literature is provided both for the elastic behaviour of a few rubber materials and for the plastic response of a typical glassy polymer like polycarbonate.

2. IMPROVED NETWORK MODELS FOR RUBBER ELASTICITY

The development of molecular orientation in rubber-like materials under deformation has been extensively studied, often by measuring the optical anisotropy or birefringence. Various deformation schemes have been proposed, based on the standard conception of a vulcanized rubber as an assembly of molecules linked together at well-defined junction points (points of vulcanization or cross-linking). One of the simple schemes is the so-called affine model, which is based on two key assumptions: (i) statistical fluctuations of the position of the junction points about their mean position can be neglected, (ii) the end-to-end vector of a chain (between junction points) co-deforms with the local deformation of the continuum it is embedded in. According to this scheme, as deformation progresses each chain stretches while rotating towards a preferred direction. At all stages each chain attempts to maximize its entropy by disorienting the elements or random links, subject only to the constraints imposed by the end-to-end vectors.

It is to be noted here that in the traditional application to purely elastic rubber-like materials, the affine deformation assumption literally implies that the end-to-end vectors deform as material lines on the continuum. In this paper we shall also be concerned with the application to molecular networks in glassy polymers in which case the network distortion will not follow the continuum deformation exactly. Nevertheless, there will be a connection between the two, but in order to keep the discussion concise, we may, for the time being, distinguish between the deformations of the network and the continuum, respectively, thus allowing for these deformations to be instantaneously different. The precise link between the two depends on the application

of the network model; this will be further discussed for rubbers in Section 2.3 and for glassy polymers in Section 3.2.

2.1. *Single chain behaviour*

We start out by briefly recapitulating the well-known non-Gaussian considerations for a single molecular chain (see e.g. Treloar, 1975). Consider a single chain between two junction points, with its end-to-end vector $\mathbf{r}_0$ in the initial state being specified by angular coordinates θ_0 and φ_0, $0 \leqslant \theta_0 \leqslant \pi$, $0 \leqslant \varphi_0 \leqslant 2\pi$, with respect to some initial frame of reference defined by the set of orthonormal base vectors $\mathbf{e}_i^0$ (see Fig. 1). If the chain contains N links of length l, the length r_0 of the unstrained free chain is given by the root-mean-square value $\sqrt{N}l$. Furthermore, consider some strained state of the chain in which the end-to-end vector $\mathbf{r}$ has length r and is oriented at angles θ and φ with respect to some current orthonormal set $\{\mathbf{e}_i\}$. In our considerations in the present and the next subsection, the two frames of references can be chosen arbitrarily; in Section 2.3 and subsequent discussions, we shall deal with the kinetics of the deformation of chains and we shall make specific identifications for $\mathbf{e}_i^0$ and $\mathbf{e}_i$, respectively. For now, it suffices to note that the stretch of the end-to-end vector in the strained state is $\lambda = r/r_0$.

By considering the statistical distribution of possible link angles at a given vector length r, Kuhn and Grün (1942) were the first to derive the configurational entropy s of the stretched chain. Their non-Gaussian chain statistics approach accounts for the finite extensibility of the chain and hence is valid for large stretches up to the limiting stretch $\lambda_L = \sqrt{N}$, even for short chains with a small value of N. Furthermore, they showed that the Helmholtz free energy w for a single chain at stretch λ (at constant absolute temperature T) is determined by the configurational entropy s through $w = -Ts$, and hence is given by

$$w = kNT\left[\frac{\lambda}{\sqrt{N}}\beta + \ln\frac{\beta}{\sinh\beta}\right] - w_0, \quad \beta = \mathscr{L}^{-1}\left(\frac{\lambda}{\sqrt{N}}\right), \tag{1}$$

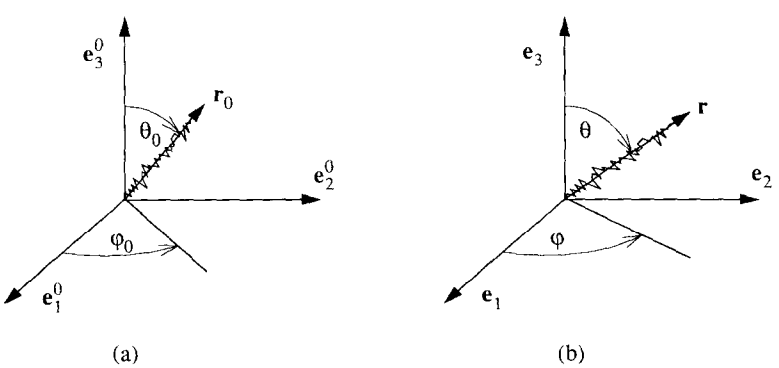

Fig. 1. A single chain in unstrained (a) and strained (b) state; definition of geometric quantities.

where w_0 is an arbitrary constant, k is Boltzmann's constant and $\mathscr{L}$ is the Langevin function defined by

$$\mathscr{L}(\beta) = \coth\beta - 1/\beta.$$

The work-rate of stress per unit volume is $\sigma\dot{\varepsilon}$ with $\dot{\varepsilon} = \dot{\lambda}/\lambda$, so that for purely elastic, isothermal deformation processes we find $\sigma\dot{\varepsilon} = \dot{w} = (\partial w/\partial\lambda)\dot{\lambda}$. Hence

$$\sigma = \lambda \frac{\partial w}{\partial \lambda}$$

with

$$\frac{\partial w}{\partial \lambda} = \frac{kT}{\sqrt{N}} \mathscr{L}^{-1}\left(\frac{\lambda}{\sqrt{N}}\right). \tag{2}$$

2.2. *The chain orientation distribution function*

Now consider a network of molecular chains with a random distribution of the orientation of their end-to-end vector $\mathbf{r}_0$ in the unstrained state. Each individual chain is described as discussed above. The deformation of the network is assumed to be homogeneous in the sense that all chains are assumed to be subjected to the same network deformation tensor. The adjective "network" is used here, as mentioned before, to emphasize that in this subsection we shall be concerned only with the network and not with the continuum in which it is embedded.

We will assume that the number of the chains per unit volume, n, is large. In effect, for characterizing the distribution of the chain orientations and stretches, we will make the transition to a continuum-like network model by considering the limiting case of an infinite number of chains. Hence, we can identify a continuous distribution of chain orientations. A so-called molecular Chain Orientation Distribution Function (CODF), denoted by $C(\theta, \varphi; t)$, is now introduced such that the relative density of molecular chains whose **r**-vector orientation at some instant t, falls in the range between (θ, φ) and $(\theta+\mathrm{d}\theta, \varphi+\mathrm{d}\varphi)$ is given by $C(\theta, \varphi; t)\sin\theta\,\mathrm{d}\theta\,\mathrm{d}\varphi$. Note that $\sin\theta\,\mathrm{d}\theta\,\mathrm{d}\varphi$ is the area on a unit sphere spanned by the interval $(\mathrm{d}\theta, \mathrm{d}\varphi)$ and that t is a time-like parameter. The actual number of chains between (θ, φ) and $(\theta+\mathrm{d}\theta, \varphi+\mathrm{d}\varphi)$ then is

$$\mathrm{d}n = nC(\theta, \varphi; t)\sin\theta\,\mathrm{d}\theta\,\mathrm{d}\varphi. \tag{3}$$

For a virgin, unstrained material the orientation of network chains can usually be considered to be distributed in a random fashion initially; then C will be independent of θ and φ, and the material's response is instantaneously isotropic. When the material is deformed all chains are stretched and, at the same time, rotated as will be shown in detail later. Hence, the CODF will develop into a nonuniform distribution, which may be quite severe, as will also be demonstrated later. Thus, texture development in the sense of molecular chain distributions is described in this model in terms of this CODF.

By definition,

$$\int_{\theta=0}^{\pi}\int_{\varphi=0}^{2\pi} C(\theta,\varphi;t)\sin\theta\,\mathrm{d}\theta\,\mathrm{d}\varphi = 1, \tag{4}$$

so that a uniform distribution, corresponding to isotropic properties, is characterized by $C(\theta,\varphi;t) = C_0 = 1/4\pi$. During the deformation process of the network, the CODF is subject to continuous change and this evolution is governed by a continuity equation in orientation space which we will now derive.

Consider an arbitrary surface region Ω of a unit sphere bounded by the curve Γ, fixed in space (see Fig. 2). The conservation law is expressed in the form that the rate at which the number of chains contained in Ω increases is equal to the rate at which chains enter into Ω over its boundary Γ:

$$\int\int_{\Omega}\frac{\partial(C\sin\theta)}{\partial t}\,\mathrm{d}\theta\,\mathrm{d}\varphi + \oint_{\Gamma}(C\sin\theta)\mathbf{v}\cdot\mathbf{n}\,\mathrm{d}\Gamma = 0, \tag{5}$$

where $\partial(C\sin\theta)/\partial t$ is the rate of increase of $(C\sin\theta)$ at a fixed point in Ω, $\mathbf{v}$ denotes the vector $(\dot\theta,\dot\varphi)$ in (θ,φ)-space, $\mathbf{n}$ denotes the outward unit normal to Γ and a $\cdot$ denotes the inner product of vectors. Rewriting the contour integral and applying Green's theorem gives

$$\oint_{\Gamma}(C\sin\theta)\mathbf{v}\cdot\mathbf{n}\,\mathrm{d}\Gamma = \int\int_{\Omega}\left[\frac{\partial(C\sin\theta\dot\theta)}{\partial\theta} + \frac{\partial(C\sin\theta\dot\varphi)}{\partial\varphi}\right]\mathrm{d}\theta\,\mathrm{d}\varphi. \tag{6}$$

Combining (5) and (6), we obtain the continuity equation for the CODF by a standard argument:

$$\frac{\partial(C\sin\theta)}{\partial t} + \frac{\partial(C\sin\theta\dot\theta)}{\partial\theta} + \frac{\partial(C\sin\theta\dot\varphi)}{\partial\varphi} = 0. \tag{7}$$

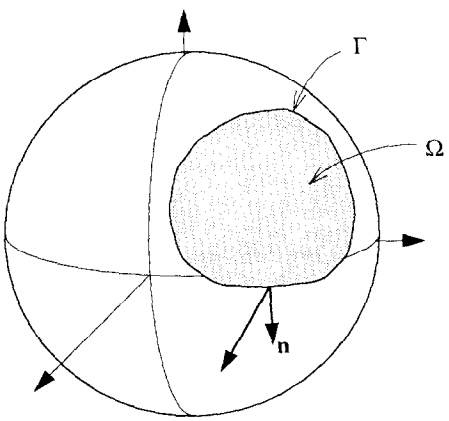

Fig. 2. A surface region Ω with boundary Γ on a unit sphere in orientation space. The increase of the volume fraction of chains per unit time within Ω must be balanced with the outflow over the boundary Γ [see (5)].

Equation (7) describes the change in the CODF at a given point in orientation space at which a number of chains is moving in orientation space. Using standard terminology of continuum mechanics, the derivation above can be referred to as an Eulerian formulation. Alternatively, we can give a Lagrangian treatment in which we follow the motion of one and the same set of chains through orientation space.

By applying the standard transformation procedure in multi-dimensional integration, the left-hand side of (4) can be written in terms of the initial orientation (θ_0, φ_0) as

$$\int_0^{\pi}\int_0^{2\pi} C \sin\theta \, d\theta \, d\varphi = \int_0^{\pi}\int_0^{2\pi} C(\theta, \varphi; t) \sin\theta J \, d\theta_0 \, d\varphi_0,$$

where in the right-hand side,

$$\theta = \theta(\theta_0, \varphi_0; t), \quad \varphi = \varphi(\theta_0, \varphi_0; t),$$

$$J = \left| \frac{\partial(\theta, \varphi)}{\partial(\theta_0, \varphi_0)} \right| = \frac{\partial\theta}{\partial\theta_0}\frac{\partial\varphi}{\partial\varphi_0} - \frac{\partial\theta}{\partial\varphi_0}\frac{\partial\varphi}{\partial\theta_0}. \tag{8}$$

On the other hand, we may also assume a given initial orientation distribution C_0, so that from the balance law (4) we have

$$\int_0^{\pi}\int_0^{2\pi} C \sin\theta \, d\theta \, d\varphi = \int_0^{\pi}\int_0^{2\pi} C_0 \sin\theta_0 \, d\theta_0 \, d\varphi_0.$$

Therefore, we obtain the relationship

$$C(\theta, \varphi; t) = C_0 \frac{\sin\theta_0}{\sin\theta} J^{-1}. \tag{9}$$

The Eulerian and Lagrangian interpretations of the motion of chains in orientation space can be made more explicit by defining a convective time derivative $\mathrm{D}/\mathrm{D}t$ in addition to the local derivative $\partial/\partial t$ appearing in (5) and (7). By analogy to the convective or material time derivative in continuum mechanics, we define

$$\frac{\mathrm{D}}{\mathrm{D}t} = \frac{\partial}{\partial t} + \dot{\theta}\frac{\partial}{\partial\theta} + \dot{\varphi}\frac{\partial}{\partial\varphi}, \tag{10}$$

so that for any arbitrary quantity f,

$$\frac{\mathrm{D}f}{\mathrm{D}t}(\theta, \varphi; t) = \frac{\partial}{\partial t} f(\theta(\theta_0, \varphi_0; t), \varphi(\theta_0, \varphi_0; t); t). \tag{11}$$

The convective derivative $\mathrm{D}f/\mathrm{D}t$ can be interpreted simply as the rate of change of the quantity f as measured by an observer travelling with the chains in orientation space. With this definition, the local continuity condition (7) for the CODF can be rewritten as

$$\frac{\mathrm{D}(C\sin\theta)}{\mathrm{D}t}+C\sin\theta\left[\frac{\partial\dot{\theta}}{\partial\theta}+\frac{\partial\dot{\varphi}}{\partial\varphi}\right]=0, \tag{12}$$

while the integral condition (5) becomes

$$\frac{\mathrm{D}}{\mathrm{D}t}\int\int_{\Omega}C\sin\theta\,\mathrm{d}\theta\,\mathrm{d}\varphi=0.$$

Recalling the definition of C, the total value F of some quantity f associated with individual chains in some orientation is given by

$$F=\int\int_{\Omega}fC\sin\theta\,\mathrm{d}\theta\,\mathrm{d}\varphi.$$

For future reference, we note that the rate of change of F can be conveniently expressed as

$$\frac{\mathrm{D}F}{\mathrm{D}t}=\int\int_{\Omega}\frac{\mathrm{D}f}{\mathrm{D}t}C\sin\theta\,\mathrm{d}\theta\,\mathrm{d}\varphi \tag{13}$$

in terms of the convective derivative. The proof is fully similar to that of Reynold's transport theorem in continuum mechanics and will not be elaborated further.

2.3. *Full network model—Eulerian form*

In this section, we shall further elaborate on the network in rubber-like materials, where the network deformation can be regarded to coincide at each moment with the continuum deformation in which it is embedded. Thus, when the material is subject to some three-dimensional deformation process represented by the deformation gradient tensor $\mathbf{F}$, each chain's end-to-end vector $\mathbf{r}_0$ is taken to be distorted (i.e. strained) and rotated to the vector $\mathbf{r}$ in an affine manner, i.e. $\mathbf{r}=\mathbf{F}\mathbf{r}_0$. The associated principal stretches λ_i $(i=1,\ldots,3)$ as well as the corresponding Lagrangian principal directions $\mathbf{e}_i^0$ in the undeformed configuration and the Eulerian principal directions $\mathbf{e}_i$ in the current deformed configuration are defined through

$$\mathbf{C}\mathbf{e}_i^0=\lambda_i^2\mathbf{e}_i^0 \quad \text{(no sum)}, \quad \mathbf{C}=\mathbf{F}^{\mathrm{T}}\mathbf{F} \tag{14}$$

and

$$\mathbf{B}\mathbf{e}_i=\lambda_i^2\mathbf{e}_i \quad \text{(no sum)}, \quad \mathbf{B}=\mathbf{F}\mathbf{F}^{\mathrm{T}}, \tag{15}$$

respectively. Here, $\mathbf{C}$ and $\mathbf{B}$ are the usual right and left Cauchy–Green tensors, respectively. In the sequel it will be extremely convenient to identify the frames of reference for the chain orientations (θ_0, φ_0) and (θ, φ) in the initial and strained state, by these Lagrangian and Eulerian triads $\mathbf{e}_i^0$ and $\mathbf{e}_i$, respectively.

It is assumed that no volume change takes place during deformation of the network and hence of the continuum. Furthermore, intermolecular interactions and changes in internal energy are neglected during the deformation. Accordingly, the total free

energy W for the network is given simply by the sum of the free energies w of the individual chains, i.e.

$$W = \int w \, \mathrm{d}n,$$

with w according to (2) and $\mathrm{d}n$ being the actual number of chains whose $\mathbf{r}$-vector orientation falls in the range of (θ, φ) and $(\theta + \mathrm{d}\theta, \varphi + \mathrm{d}\varphi)$. According to (3), W can be expressed in the terms of the CODF as given by

$$W = n \int_0^{\pi} \int_0^{2\pi} wC(\theta, \varphi; \lambda_i) \sin\theta \, \mathrm{d}\theta \, \mathrm{d}\varphi. \tag{16}$$

Here, we have substituted the principal stretches as the time-like parameter t in the previous expressions for the CODF. This is possible since, as a consequence of the affine deformation assumption, the distortion of the network is independent of the rate of deformation, so that t only needs to be some monotonic parameter. Identifying t with λ_i will turn out to be convenient for further development.

Expression (16) shows that due to the affine deformation assumption and the isotropy of the initial orientation distribution of the chain vectors $\mathbf{r}_0$, the total free energy W for the network can be expressed solely as a function of the principal stretches λ_i. By a standard argument (see, e.g. OGDEN, 1984), it then follows that the principal axes of the Cauchy stress tensor $\boldsymbol{\sigma}$ coincide with the Eulerian triad $\{\mathbf{e}_i\}$, so that

$$\boldsymbol{\sigma} = \sum_i \sigma_i (\mathbf{e}_i \otimes \mathbf{e}_i) \tag{17}$$

with the principal stresses σ_i required to sustain the imposed deformation being determined by the gradient of W in λ_i-space. Recalling the exposition in the previous subsection, the convective derivative $\mathrm{D}/\mathrm{D}t$ is the appropriate rate of change of any chain-associated quantity. After identifying t with λ_i again, the appropriate gradient in this paper is $\mathrm{D}/\mathrm{D}\lambda_i$ so that we obtain

$$\sigma_i = \lambda_i \frac{\mathrm{D}W}{\mathrm{D}\lambda_i} - p \quad \text{(no sum)}. \tag{18}$$

Here, p is an additional hydrostatic pressure which is left indeterminate by the free energy function because of incompressibility, $\lambda_1 \lambda_2 \lambda_3 = 1$, but which is determined from the boundary conditions. With the total free energy W being given by (16), we obtain according to (13)

$$\frac{\mathrm{D}W}{\mathrm{D}\lambda_i} = n \int_0^{\pi} \int_0^{2\pi} \frac{\mathrm{D}w}{\mathrm{D}\lambda_i} C \sin\theta \, \mathrm{d}\theta \, \mathrm{d}\varphi. \tag{19}$$

We now proceed by deriving the expressions for w and the CODF C as a function of the principal stretches that need to be substituted into (19). To that end, we consider the distortion of an initial chain end-to-end vector $\mathbf{r}_0$ into the end-to-end vector $\mathbf{r}$ in

the current state. The components of the associated unit direction vectors $\mathbf{m} = \mathbf{r}/r = m_i\mathbf{e}_i$ in current state, and $\mathbf{m}_0 = \mathbf{r}_0/r_0 = m_i^0\mathbf{e}_i^0$ in the initial state are (see Fig. 1)

$$m_1 = \sin\theta\cos\varphi, \quad m_2 = \sin\theta\sin\varphi, \quad m_3 = \cos\theta, \tag{20}$$

and

$$m_1^0 = \sin\theta_0\cos\varphi_0, \quad m_2^0 = \sin\theta_0\sin\varphi_0, \quad m_3^0 = \cos\theta_0, \tag{21}$$

respectively. Invoking the affine deformation assumption, $\mathbf{r} = \mathbf{F}\mathbf{r}_0$, and the well-known continuum mechanics relationship $\mathbf{F}\mathbf{e}_i^0 = \lambda_i\mathbf{e}_i$ (no sum), the components of the unit direction vectors $\mathbf{m}$ and $\mathbf{m}_0$ on the Lagrangian and Eulerian bases respectively, are inter-related by

$$m_i = \frac{\lambda_i}{\lambda}m_i^0 \tag{22}$$

or

$$\sin\theta\cos\varphi = \frac{\lambda_1}{\lambda}\sin\theta_0\cos\varphi_0,$$

$$\sin\theta\sin\varphi = \frac{\lambda_2}{\lambda}\sin\theta_0\sin\varphi_0,$$

$$\cos\theta = \frac{\lambda_3}{\lambda}\cos\theta_0. \tag{23}$$

Furthermore, one may invoke $\mathbf{r} = \mathbf{F}\mathbf{r}_0$ so as to eliminate $\mathbf{r}$ from the expression $\lambda^2 = r^2/r_0^2 = (\mathbf{r}\cdot\mathbf{r})/(\mathbf{r}_0\cdot\mathbf{r}_0)$, such that the stretch λ can be written as $\lambda^2 = \mathbf{m}_0\cdot\mathbf{C}\cdot\mathbf{m}_0$. Introducing then the components of $\mathbf{m}_0$ on the Lagrangian triad $\mathbf{e}_i^0$ gives, with the aid of (14),

$$\lambda^2 = \sum_i (m_i^0)^2\lambda_i^2. \tag{24}$$

This expression determines the stretch λ of a single chain as a function of its initial orientation, i.e. λ is found as a function $\lambda(\theta_0, \varphi_0; \lambda_i)$. Similarly, by starting out from $\lambda^{-2} = (\mathbf{r}_0\cdot\mathbf{r}_0)/(\mathbf{r}\cdot\mathbf{r})$, one finds

$$\lambda^{-2} = \sum_i m_i^2/\lambda_i^2, \tag{25}$$

which governs the stretch as a function of the current chain orientation, i.e. $\lambda = \lambda(\theta, \varphi; \lambda_i)$.

With either one of these relations for λ as a function of λ_i, the free energy function w to be substituted into (19) can be formally constructed. However, one may note that

$$\frac{\mathrm{D}w}{\mathrm{D}\lambda_i} = \frac{\partial w}{\partial\lambda}\frac{\mathrm{D}\lambda}{\mathrm{D}\lambda_i},$$

where $\partial w/\partial\lambda$ is immediately given by (2) and where, according to the definition of the derivative $\mathrm{D}/\mathrm{D}\lambda_i$, the term $\mathrm{D}\lambda/\mathrm{D}\lambda_i$ is the partial derivative of λ as a function $\lambda(\theta_0, \varphi_0; \lambda_i)$. This function is determined by (25), and after differentiation and elimination of m_i^0 by means of (22), one finds $\mathrm{D}\lambda/\mathrm{D}\lambda_i = (\lambda/\lambda_i)m_i^2$. Hence,

$$\frac{\mathrm{D}W}{\mathrm{D}\lambda_i} = nkT\sqrt{N}\int_0^{\pi}\int_0^{2\pi} C\mathscr{L}^{-1}\left(\frac{\lambda}{\sqrt{N}}\right)\lambda\frac{m_i^2}{\lambda_i}\sin\theta\,\mathrm{d}\theta\,\mathrm{d}\varphi,$$

and the principal stresses, according to (18), can be written as

$$\sigma_i = C^{\mathrm{R}}\sqrt{N}\int_0^{\pi}\int_0^{2\pi} C\mathscr{L}^{-1}\left(\frac{\lambda}{\sqrt{N}}\right)\lambda m_i^2\sin\theta\,\mathrm{d}\theta\,\mathrm{d}\varphi - p, \tag{26}$$

where $C^{\mathrm{R}} = nkT$ is known as the rubber modulus.

The final step now is the derivation of the solution for the CODF $C = C(\theta, \varphi; \lambda_i)$. With the help of (20), (23), (25) and (8), the CODF can now be explicitly determined from (9) by a very long but straightforward calculation, which results in the following general expression:

$$C(\theta, \varphi; \lambda_i) = C_0\lambda^3(\theta, \varphi; \lambda_i), \tag{27}$$

where $C_0 = 1/4\pi$ is the initial uniform distribution and where $\lambda(\theta, \varphi; \lambda_i)$ is to be solved from (25). Substituting (27) into (26), we finally obtain the principal stresses as

$$\sigma_i = \frac{1}{4\pi}C^{\mathrm{R}}\sqrt{N}\int_0^{\pi}\int_0^{2\pi}\mathscr{L}^{-1}\left(\frac{\lambda}{\sqrt{N}}\right)\lambda^4 m_i^2\sin\theta\,\mathrm{d}\theta\,\mathrm{d}\varphi - p. \tag{28}$$

Once these principal stresses are evaluated, the stress tensor $\boldsymbol{\sigma}$ itself is constructed by application of (17).

2.4. *Full network model—Lagrangian form*

The full network model we derived in the above can also be developed in the initial configuration, i.e. in a Lagrangian form. There are two different ways to arrive at this. One is an approach based on the initial, uniform chain orientation distribution as demonstrated by Wu and Van der Giessen (1992). The other, which we will now derive, employs a transformation of (28).

The principal stresses in the form (26) can be directly transformed to the initial configuration:

$$\sigma_i = C^{\mathrm{R}}\sqrt{N}\int_0^{\pi}\int_0^{2\pi} C\mathscr{L}^{-1}\left(\frac{\lambda}{\sqrt{N}}\right)\lambda\frac{\lambda_i^2(m_i^0)^2}{\lambda^2}\sin\theta J\,\mathrm{d}\theta_0\,\mathrm{d}\varphi_0 - p$$

with J according to (8). By noting (9) or $C\sin\theta J = C_0\sin\theta_0 = (1/4\pi)\sin\theta_0$, we finally obtain

$$\sigma_i = \frac{1}{4\pi} C^R \sqrt{N} \int_0^{\pi} \int_0^{2\pi} \mathscr{L}^{-1}\left(\frac{\lambda}{\sqrt{N}}\right) \frac{\lambda_i^2 (m_i^0)^2}{\lambda} \sin\theta_0 \, d\theta_0 \, d\varphi_0 - p \tag{29}$$

with $\lambda = \lambda(\theta_0, \varphi_0; \lambda_i)$ calculated from (24).

Equations (29) are exactly as derived previously by the authors (WU and VAN DER GIESSEN, 1992). As pointed out in that paper, the equations (29) are similar to those given by TRELOAR and RIDING (1979). However, TRELOAR and RIDING (1979) limited their attention to (i) biaxial deformation, and (ii) deformations with fixed principal axes of stretching so that the Eulerian and Lagrangian triads retained fixed orientations in space. The present formulation is valid for arbitrary three-dimensional deformations; for the biaxial deformations mentioned, the model reduces to that in TRELOAR and RIDING (1979).

It will be noted that in this Lagrangian approach, the CODF is not needed at all for the computation of the network stresses. This is an obvious advantage when one is only interested in the stress–strain response. However, the CODF in itself is an essential source of information about the actual orientation distribution of molecular chains at any stage of a general three-dimensional state of deformation, which the authors have not found before in the literature.

2.5. *Simplified models*

In the present paper, we shall consider two simplified network models that have been proposed in the literature, namely the three-chain model and the eight-chain model. The three-chain model was originally suggested by JAMES and GUTH (1943) and assumes that a network containing n chains per unit volume is equivalent to three independent (non-interacting) sets of $n/3$ chains per unit volume parallel to the Eulerian principal axes as shown in Fig. 3(a). The principal values of the stress tensor according to this model are

$$\sigma_i^{3\text{-ch}} = \frac{1}{3} C^R \sqrt{N} \lambda_i \mathscr{L}^{-1}\left(\frac{\lambda_i}{\sqrt{N}}\right) - p. \tag{30}$$

The eight-chain model was proposed by ARRUDA and BOYCE (1991, 1992a) and considers a set of eight chains connecting the central junction point and each of eight

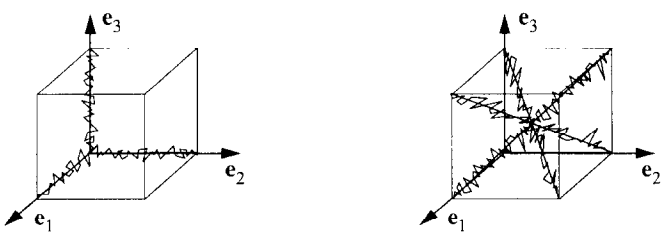

FIG. 3. Schematic representation of the three-chain model (a) and the eight-chain model (b).

corners of the unit cube as shown in Fig. 3(b). The principal values of the stress tensor according to this model are given by

$$\sigma_i^{8\text{-ch}} = \frac{1}{3} C^R \sqrt{N} \frac{\lambda_i^2}{\lambda} \mathscr{L}^{-1}\left(\frac{\lambda}{\sqrt{N}}\right) - p, \tag{31}$$

with

$$\lambda^2 = \frac{1}{3}\sum_i \lambda_i^2.$$

Comparing these three- and eight-chain samplings with the actual three-dimensional initial random distribution of molecular chains, we expected that the three-chain model would be likely to overestimate the actual stiffness of the network, while the eight-chain representation would probably give a lower bound (Wu and Van der Giessen, 1992). Indeed, as will be demonstrated in the next section, the stress response predicted by our full network model (28) or (29) is for the same value of N and C^R always in-between that predicted by the three-chain model and eight-chain model, respectively. However, the integrations involved in (28) and (29) require a rather time-consuming numerical procedure (see Section 2.6), which is certainly not appealing when one wishes to incorporate the model in, for instance, finite element computations. All these observations motivated us to search for an approximation of the full integration by combining the three-chain and eight-chain models. One possibility is a simple linear combination,

$$\sigma_i = (1-\rho)\sigma_i^{3\text{-ch}} + \rho\sigma_i^{8\text{-ch}}, \tag{32}$$

where the parameter ρ may be a constant or related to some other physical quantity which is, for instance, related to the deformation process. In our previous paper (Wu and Van der Giessen, 1992), ρ was proposed to be related to the maximal principal stretch $\lambda_{max} = \max(\lambda_1, \lambda_2, \lambda_3)$ by

$$\rho = 0.85\lambda_{max}/\sqrt{N}, \tag{33}$$

where the factor 0.85 was chosen to give the best correlation with full integration of (28) or (29). In this way, the eight-chain contribution in (32) becomes increasingly important when λ_{max} approaches the limit stretch $\lambda_L = \sqrt{N}$ of a single chain.

2.6. *Results*

Before considering the stress responses according to the network models described in the above, we shall first study the distortion of the network during a few deformation processes in terms of the CODF. As mentioned before, the CODF gives the precise spatial distribution of the chain orientations for an arbitrary three-dimensional deformation, and thus provides key information about the anisotropy of chain associated quantities. Also, this will provide important hindsight to appreciate the simplified network models later on.

Equation (27) is the general expression for the CODF in the current orientation space (θ, φ) relative to the Eulerian triad at given values of the principal stretches λ_i,

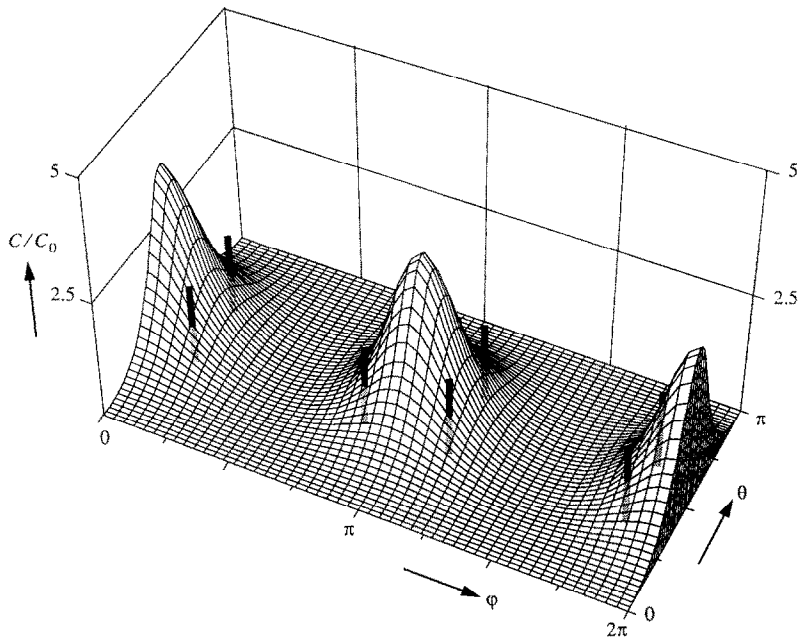

FIG. 4. Three-dimensional plot of the CODF during uniaxial tension along the $\mathbf{e}_1$ direction for a stretch of $\lambda = 1.5$. The vertical bars indicate the orientation of the chains in the eight-chain model.

with the function $\lambda(\theta, \varphi; \lambda_i)$ to be solved from (25). Figures 4 and 5 show the CODF during uniaxial extension at various stages of the applied stretch λ. In that case, the Eulerian triad retains fixed directions in space and the principal stretches are $\lambda_1 = \lambda$, $\lambda_2 = \lambda_3 = \lambda^{-1/2}$. The three-dimensional plot in Fig. 4 gives a complete picture of the

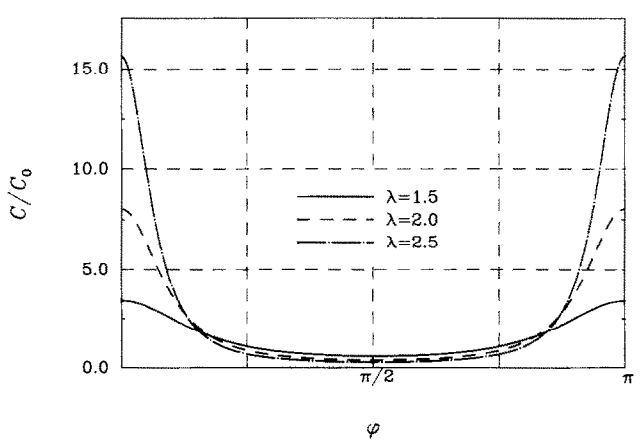

FIG. 5. Plane section of the CODF at $\theta = \pi/2$ during uniaxial tension (cf. Fig. 4) at various levels of the stretch λ.

spatial chain orientation at a stretch of $\lambda = 1.5$. The molecular texture created during this deformation due to the stretching out and simultaneous rotation of the chains is clearly seen as two distinct peaks in the CODF in the stretching direction $\mathbf{e}_1$, i.e. $\varphi = 0$, $\theta = 0$ or $\theta = \pi$. As stretching continues, these peaks become increasingly intense, as shown in Fig. 5 in a two-dimensional section of the CODF in the $\mathbf{e}_1$–$\mathbf{e}_2$ plane ($\theta = \pi/2$) for various stretches. It will appear to be instructive to compare the actual spatial chain distribution with the three-chain and eight-chain approximations. In the three-chain model of Fig. 3(a), the network is represented by three effective chains along the three principal directions, where the one along the tensile stretch direction $\mathbf{e}_1$ will have to carry the tensile stress. Thus, this single chain should represent the actual cloud of chains around this preferred direction as shown in Figs 4 and 5, a large fraction of which do not quite have that preferred direction and will contribute less to the axial stiffness. Shown explicitly in Fig. 4 is the orientation of the eight chains in the eight-chain model of Fig. 3(b) at the current stretch level, which is readily obtained from the expressions (23) and (24). It is seen that these orientations have rotated towards the actual CODF peaks with ongoing deformation, but are considerably off the ideal orientation. This implies that any chains that are oriented close to the ideal orientation, and which therefore will carry most of the load, are not taken into account in the eight-chain model.

Next, we consider the case of simple (and *not* pure) shear, where the deformation gradient is given by the components

$$[F_{ij}] = \begin{bmatrix} 1 & \gamma & 0 \\ 0 & 1 & 0 \\ 0 & 0 & 1 \end{bmatrix}$$

with respect to some global Cartesian basis $\{\mathbf{g}_i\}$. In this case, the Eulerian strain triad $\{\mathbf{e}_i\}$ does not retain a fixed orientation in space, but the $\mathbf{e}_1$–$\mathbf{e}_2$ axes are inclined with respect to the $\mathbf{g}_1$–$\mathbf{g}_2$ axes at an angle $\alpha = (\pi/4) + (1/2)\arctan(\gamma/2)$. The actual spatial orientation in the $\mathbf{g}_1$–$\mathbf{g}_2$ plane is therefore given by the angle $\Phi = \alpha + \varphi$, and this angle is used to plot the section of the CODF in that plane ($\theta = \pi/2$) as shown in Fig. 6. It is observed that molecular orientation effects now lead to the development of strong CODF peaks at the principal stretch orientations (i.e. for $\varphi = 0$) which, in addition, rotate towards the final orientation $\Phi = \alpha = 0$ for the shear $\gamma \to \infty$.

We shall now proceed by considering the stress–strain response according to the models discussed above. The principal stresses according to the full network model are given by either the Eulerian expression (28) or the Lagrangian form (29). At each stage of the deformation, the double integrals in these expressions are evaluated by first noting that due to symmetry only the intervals $\theta \in [0, \pi/2]$, $\varphi \in [0, \pi/2]$ need to be considered, then subdividing that area into a number of cells and integrating within each cell using Gaussian quadrature. This procedure is basically equivalent to that described by TRELOAR and RIDING (1979). Recursive refinement is applied for each cell until the integral is obtained within a relative error of 10^{-5}. The Eulerian and Lagrangian expressions (28) and (29), respectively, are mathematically equivalent, but it turns out that the evaluation of the integrals in the Eulerian expression is much more time-consuming than the Lagrangian one because the integrand is a significantly more nonlinear function of θ and φ.

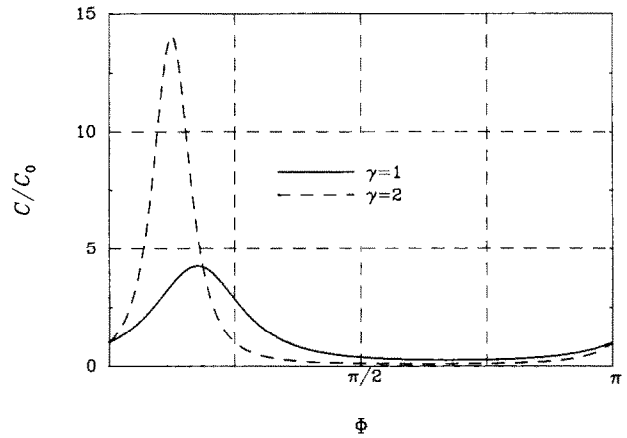

FIG. 6. Plane section of the CODF at $\theta = \pi/2$ during plane simple shear at two stages of the deformation.

Figure 7 shows the predicted response to uniaxial extension in the $\mathbf{e}_1$ direction with principal stretches $\lambda_1 = \lambda$, $\lambda_2 = \lambda_3 = \lambda^{-1/2}$, as discussed above. The principal tensile stress is $\sigma_1 = \sigma$, while the conditions $\sigma_2 = \sigma_3 = 0$ are used to determine the unknown pressure p in the constitutive relations (28)–(31). Contrary to Wu and van der Giessen (1992) who presented the results in terms of the true stress σ, we here show the nominal stress f or load per unit undeformed area, which is in this case simply given by $f = \sigma\lambda_2\lambda_3 = \sigma/\lambda$. Figure 7 shows the results according to the full network model as well as the simplified three-chain and eight-chain models. The values $N = 75$ and $C^R = 0.273$ MPa were used for all three models; they were simply used as

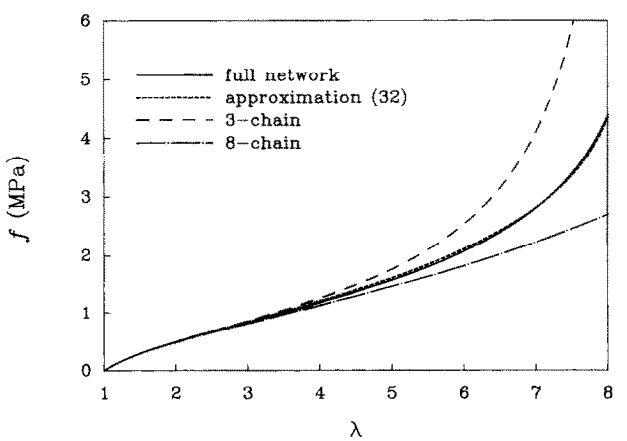

FIG. 7. Predicted load vs stretch diagram for uniaxial tension according to different network models with $N = 75$ and $C^R = 0.273$ MPa.

representative values of N and C^R, and were given by TRELOAR (1975) for uniaxial tension of a vulcanized rubber. All models considered correctly predict a typical S-shaped load vs stretch curve exhibited by rubber materials. What this result clearly shows is that relative to the full network model, the three-chain approximation tends to overestimate the stiffness at large stretches, while the eight-chain model tends to underestimate. There is no significant difference up to stretches of $\lambda \approx 3$ (or roughly 30% of the limit stretch). The difference at larger stretches seems to be associated with the different limit stretches of the complete network. The stretching according to the three-chain model is limited directly by the limit tensile stretch $\lambda_L = \sqrt{N}$ of the chains parallel to the tensile direction, while the overall network limiting stretch for the eight-chain model exceeds λ_L. It is seen that the approximate expression (32) for the full network response is indeed very accurate up to very large stretches.

A more important aspect appears to be the description of the network response under different states of deformation. Indeed, the primary motivation for the introduction of the eight-chain model by ARRUDA and BOYCE (1991) was the observation that the standard three-chain model could not pick up the dependence of the state of deformation observed experimentally in rubber materials. In order to assess the accuracy with which the three- and eight-chain models can account for the state of deformation dependence, ARRUDA and BOYCE (1992a) took the following procedure. For a given model, the network parameters N and C^R for a certain material are fitted from uniaxial tension or compression data, and are then used to predict other deformation processes like equi-biaxial tension or plane strain compression. Here, we shall follow a similar procedure but now for the simplified models in comparison with the full network model. Our procedure will be slightly different in the sense that we shall not fit C^R and N independently, but we shall use one value of C^R for all three models. The motivation for this is that the small strain behaviour is governed primarily by C^R, while the network models virtually coincide at these strains (and in fact approach the Gaussian network model). The various network predictions differ essentially only at relatively large strains, and the values of N will be fitted in that range. We shall apply this for two materials and two classes of deformations, as shown in Figs 8 and 9, respectively.

Figure 8 shows results for uniaxial and biaxial tension of a natural-rubber gum as reported by JAMES *et al.* (1975). The (equi-) biaxial stretching is characterized by the principal stretches $\lambda_1 = \lambda_2 = \lambda$, $\lambda_3 = \lambda^{-2}$ along fixed directions, while the material is in a state of plane stress, i.e. $\sigma_3 = 0$. The figures show the loads in the stretching directions, i.e. $f = \sigma_1/\lambda$ for uniaxial tension and $f = \sigma_1/\lambda = \sigma_2/\lambda$ for biaxial tension. The Figs 8(a)–(c) show results for the three-chain, eight-chain and full network models, respectively, where in each case the value $C^R = 0.4$ was used while the value of N was fitted for each model to the uniaxial data. It is observed that the three-chain model [see Fig. 8(a)] cannot predict the significantly different behaviour in biaxial tension, especially at larger stretches. The eight-chain model does predict a stiffer response in biaxial tension at larger stretches, but still underestimates the experimental data [see Fig. 8(b)]. Notice that the value of N for the eight-chain model is about three times smaller than that for the three-chain model. These conclusions are similar to those found by ARRUDA and BOYCE (1992a) using similar data from TRELOAR

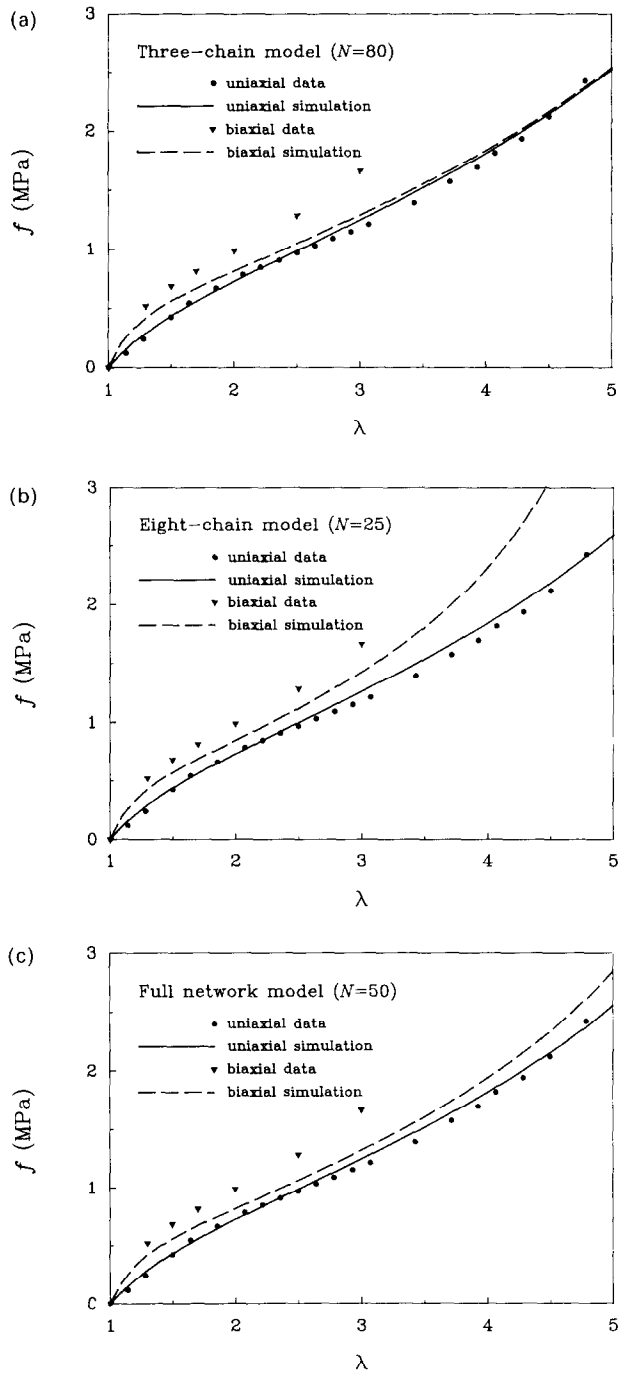

FIG. 8. Load vs stretch diagram for uniaxial and equi-biaxial tension of a natural-rubber gum for the three-chain (a), the eight-chain (b) and the full network model (c). The experimental data is taken from JAMES *et al.* (1975) and $C^R = 0.4$ MPa.

(1944) for another material. Figure 8(c) shows the results for the full network model, and it is seen that the predicted response for biaxial tension is significantly lower than the experimental data and in fact is slightly lower than that according to the eight-chain model.

The second set of cases, shown in Fig. 9, is concerned with uniaxial and plane strain compression of a silicone rubber as investigated also by ARRUDA and BOYCE (1992a). Uniaxial compression in the $\mathbf{e}_1$ direction is characterized by principal stretches $\lambda_1 = \lambda < 1$, $\lambda_2 = \lambda_3 = \lambda^{-1/2}$, while plane strain compression is determined by $\lambda_1 = \lambda < 1$, $\lambda_2 = 1$, $\lambda_3 = \lambda^{-1}$. For all three models the value $C^R = 0.435$ is used, and the value of N is for each model fitted to the uniaxial data. It is seen in Fig. 9(a) that the three-chain model overestimates the stiffness during plane strain compression for compressions $1/\lambda$ larger than about 2, while the eight-chain model is found to underestimate slightly the stress response in that regime [see Fig. 9(b)]. The plane strain compression prediction for the full network shown in Fig. 9(c) agrees well with the experimental results up to $1/\lambda \approx 2.5$ but for continued compression a softer response was found experimentally.

At this point, it should be recalled that the three- and eight-chain models are both based on approximate descriptions of an affine network model, and that our full network theory is based on the exact treatment of that concept. As suggested also by ARRUDA and BOYCE (1992a) one would expect that the full network model provides a better description of real rubber behaviour. However, we do not find that the full network model's predictions are necessarily in better agreement with experimental results than the predictions of the eight-chain model. The biaxial tension results especially of Fig. 8 are captured best by the eight-chain model. This does not imply however that the eight-chain model is a better model *per se*. There are several assumptions that underly the present network concept, and which can act as potential sources of discrepancy with experiments. First of all, there are several so-called network defects, such as unstable cross-links and interlooping of chains or entanglements, as suggested already by FLORY (1944), which may have a very significant effect. One of the key assumptions is that the junction points in the network provide permanent nodes in the network; however, molecular chains may also slide relative to each other at so-called sliplinks (see e.g. BALL *et al.*, 1981). All these network defects will tend to reduce the actual stiffness of the network. Furthermore, the affine assumption is known to hold with high accuracy at low deformations, but it has been suggested that as the deformation increases, the behaviour of a real network approaches the so-called phantom network in which the junction points move independent of the continuum (see e.g. MARK and ERMAN, 1988). Also it cannot be ruled out that at large deformations, when chains are rotated towards a common axis to such an extent that they become lined up, intermolecular interactions are no longer negligible. Molecular dynamics simulations (GAO and WEINER, 1991) seem to indicate that this may be a significant effect already at relatively small deformations in the Gaussian regime, and it may be expected to be even more important at the large strain levels considered here, leading to a more diffuse CODF than we have predicted. In conclusion, if the eight-chain model seems effective in picking up all these effects in an average sense, this is more due to coincidence than to more accurate modelling.

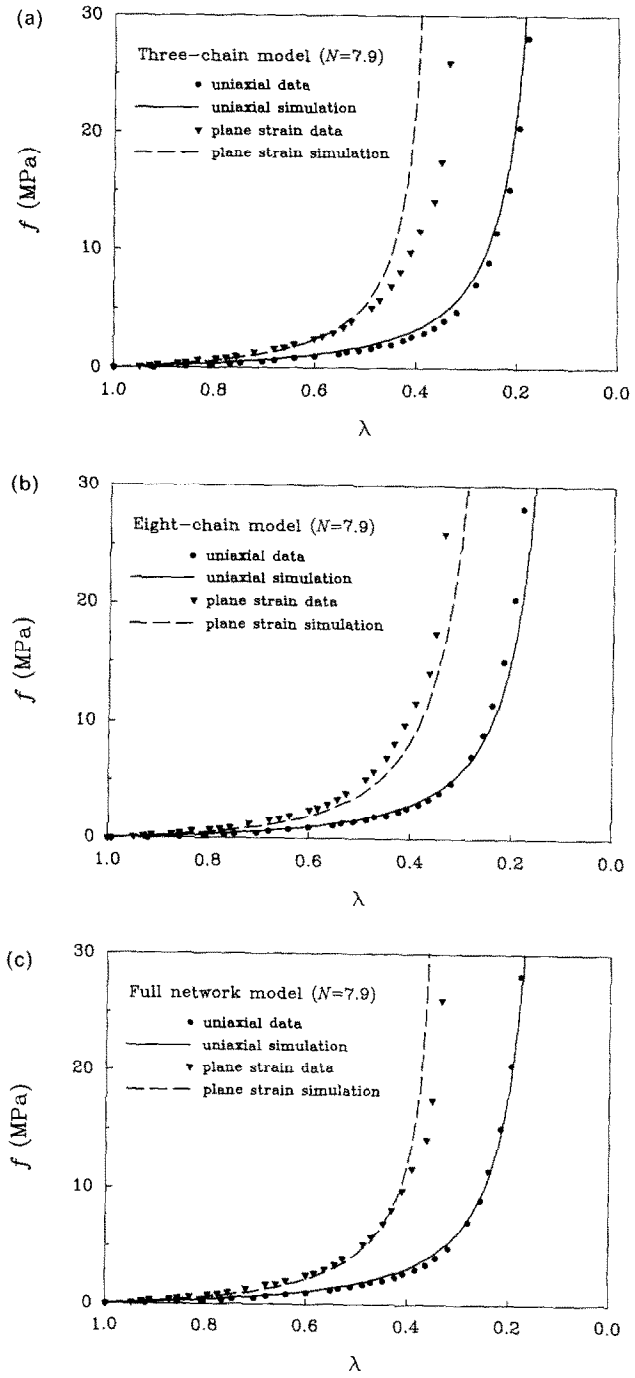

FIG. 9. Load vs stretch diagram for uniaxial and plane strain compression of a silicone rubber for the three-chain (a), the eight-chain (b) and the full network model (c). The experimental data is taken from ARRUDA and BOYCE (1992a) and $C^R = 0.435$ MPa.

3. A Large Inelastic Deformation Model for Glassy Polymers

We start by briefly recapitulating the so-called BPA model developed by Boyce *et al.* (1988). In the BPA model, the microstructure of an isotropic amorphous polymer is assumed to consist primarily of long molecular chains, which are randomly coiled in space. Side groups protrude from the backbone chains at various locations and, in conjunction with overall chain trajectory, can act as nodes, or points of physical entanglement. This results in a network-like structure much like that of rubber as discussed in Section 2, but with the chemical cross-links replaced by physical entanglements.

Following the work of Haward and Thackray (1968), it is further assumed that a glassy polymer must overcome two physically distinct sources of resistance before large strain inelastic flow may occur. Below the glass transition temperature, prior to initial yield, the material must be stressed to exceed its intermolecular resistance to segment rotation; this will be discussed first. Once the material is free to flow, molecular alignment occurs, resulting in an anisotropic internal resistance to further inelastic deformation, which is called orientational hardening; this shall be discussed in Section 3.2.

The intermolecular resistance to plastic flow is due to the impedence imposed by neighbouring chains on the ability of a chain segment to rotate either individually or in a cluster. Argon (1973) developed an expression for the plastic shear strain rate, $\dot{\gamma}^p$, which ensues once the isotropic barrier to chain segment rotation has been overcome:

$$\dot{\gamma}^p = \dot{\gamma}_0 \exp\left[-\frac{As_0}{T}\left\{1-\left(\frac{\tau}{s_0}\right)^{5/6}\right\}\right], \tag{34}$$

where $\dot{\gamma}_0$ is a pre-exponential factor, A is proportional to the activation volume/Boltzmann's constant, T is the absolute temperature and τ is the applied shear stress. Furthermore, $s_0 = 0.077\,\mu/(1-\nu)$ is the athermal shear strength, μ is the elastic shear modulus and ν is Poisson's ratio. Boyce *et al.* (1988) extended this expression to include the effects of pressure and strain softening. They used $s+\alpha p$ instead of s_0, where p is the pressure and α is the pressure dependence coefficient. Further, s is assumed to evolve with plastic straining via $\dot{s} = h(1-s/s_{ss})\dot{\gamma}^p$, where h is the rate of resistance drop with respect to the plastic strain, and s_{ss} is the assumed saturation value of s.

3.1. *Three-dimensional representation*

Consider the homogeneous deformation of an initially isotropic body loaded so that its deformation gradient at a subsequent time is $\mathbf{F}$. The deformation gradient may be multiplicatively decomposed into elastic and plastic parts, $\mathbf{F} = \mathbf{F}^e\mathbf{F}^p$. Following Lee (1969) and others, Boyce *et al.* (1988) take $\mathbf{F}^e$ to be symmetric, so that $\mathbf{F}^p$ represents the relaxed configuration obtained by unloading without rotation (in the polar decomposition sense). Hence, $\mathbf{F}^p$ can be decomposed as $\mathbf{F}^p = \mathbf{V}^p\mathbf{R}$ with the plastic stretch $\mathbf{V}^p$ and the total stretch $\mathbf{V}$ in the polar decomposition $\mathbf{F} = \mathbf{V}\mathbf{R}$ being

related by $\mathbf{V} = \mathbf{F}^e\mathbf{V}^p$. The rate quantities corresponding to this decomposition consist of the velocity gradient $\mathbf{L}$,

$$\mathbf{L} = \dot{\mathbf{F}}\mathbf{F}^{-1} = \mathbf{D}+\mathbf{W} = \dot{\mathbf{F}}^e\mathbf{F}^{e\,-1}+\mathbf{F}^e\mathbf{L}^p\mathbf{F}^{e\,-1},$$

where $\mathbf{D}$ is the strain-rate, $\mathbf{W}$ is the spin, $\mathbf{L}^p = \mathbf{D}^p+\mathbf{W}^p = \dot{\mathbf{F}}^p\mathbf{F}^{p\,-1}$ is the velocity gradient of the relaxed configuration, and where superposed dots denote the material time derivative. With the adopted symmetry of $\mathbf{F}^e$, $\mathbf{W}^p$ is algebraically given as $\mathbf{W}$ plus a term dependent on $\mathbf{F}^e$ and $\mathbf{D}+\mathbf{D}^p$. The plastic strain-rate $\mathbf{D}^p$ must be constitutively prescribed. In the BPA model, the magnitude of $\mathbf{D}^p$ is taken to be given by the plastic shear strain rate $\dot{\gamma}^p$ according to (34), while the tensor direction of $\mathbf{D}^p$ is specified by $\mathbf{N}$, so that

$$\mathbf{D}^p = \dot{\gamma}^p\mathbf{N}. \tag{35}$$

The direction $\mathbf{N}$ is the deviatoric part (indicated by a $'$) of the driving stress $\boldsymbol{\sigma}^*$ normalized by the effective equivalent shear stress τ:

$$\mathbf{N} = \frac{1}{\sqrt{2}\tau}\boldsymbol{\sigma}^{*\prime}, \quad \tau = [\tfrac{1}{2}\boldsymbol{\sigma}^{*\prime}:\boldsymbol{\sigma}^{*\prime}]^{1/2}. \tag{36}$$

The driving stress $\boldsymbol{\sigma}^*$ itself is defined by

$$\boldsymbol{\sigma}^* = \boldsymbol{\sigma} - \frac{1}{J}\mathbf{F}^e\mathbf{B}\mathbf{F}^e, \tag{37}$$

where $\boldsymbol{\sigma}$ is the Cauchy stress tensor, $\mathbf{B}$ is the back stress tensor due to strain hardening resulting from molecular alignment, and $J = \det \mathbf{F}^e$. The corresponding effective stress τ is taken to be the driving force in the plastic flow equation (34). The Cauchy stress is taken to be given by the elastic constitutive law (Anand, 1979)

$$\boldsymbol{\sigma} = \frac{1}{J}\mathbf{L}^e:[\ln \mathbf{F}^e], \tag{38}$$

where $\mathbf{L}^e$ is the usual fourth-order isotropic elastic modulus tensor. The theory needs to be complemented with constitutive equations for the back stress $\mathbf{B}$. In all computations to be presented later, the elastic strains remain small and all geometric nonlinearities associated with elastic deformations such as in (37) are neglected (see also Boyce *et al.*, 1988).

3.2. *Orientation hardening*

Once the material is stressed to the point of overcoming intermolecular barriers to chain motion, the molecular chains will be stretched and will tend to align along the direction of principal plastic stretch. This action decreases the configurational entropy of the system which, in turn, is responsible for the internal resistance to continued flow. This process of network distortion is very similar to that of rubber network, and Haward and Thackray (1968) suggested describing this for uniaxial extension by means of a back stress determined through the Langevin expression (2). Boyce *et al.* (1988) extended this approach to general three-dimensional plastic deformations

by introducing a back stress tensor $\mathbf{B}$ which is taken to be coaxial with the plastic stretch tensor $\mathbf{V}^{\mathrm{p}}$. Thus, if $\mathbf{e}_i^{\mathrm{p}}$ are the unit eigenvectors of $\mathbf{V}^{\mathrm{p}}$, the back stress $\mathbf{B}$ is constructed as

$$\mathbf{B} = \sum_i B_i(\mathbf{e}_i^{\mathrm{p}} \otimes \mathbf{e}_i^{\mathrm{p}})$$

from the principal components B_i. BOYCE *et al.* (1989) presented an extended version of their model to account for initial anisotropy; but, here we will assume that the initial network structure of the polymer is isotropic.

According to the three-chain implementation of BOYCE *et al.* (1988), the principal components of $\mathbf{B}$ can be determined from equations (30), where the λ_i are now replaced by λ_i^{p}, the principal values of the left plastic stretch tensor $\mathbf{V}^{\mathrm{p}}$. Since plastic flow according to (35) and (36) is affected only by the deviatoric part of $\boldsymbol{\sigma}^*$, we stipulate $\mathbf{B}$ to be deviatoric, so that the principal components of the back stress tensor according to this three-chain non-Gaussian network model are

$$B_i^{\text{3-ch}} = \frac{1}{3} C^{\mathrm{R}} \sqrt{N} \left[\lambda_i^{\mathrm{p}} \mathscr{L}^{-1}\left(\frac{\lambda_i^{\mathrm{p}}}{\sqrt{N}}\right) - \frac{1}{3} \sum_{j=1}^{3} \lambda_j^{\mathrm{p}} \mathscr{L}^{-1}\left(\frac{\lambda_j^{\mathrm{p}}}{\sqrt{N}}\right) \right]. \tag{39}$$

However, very recently, ARRUDA and BOYCE (1991) found that the three-chain non-Gaussian network model was not capable of picking up the strain hardening observed experimentally in polycarbonate (PC). These findings seem to have triggered their suggestion to model the network by eight equivalent chains instead of three, and very recently presented a detailed discussion and comparison with experimental results for PC and polymethylmethacrylate (PMMA) (ARRUDA and BOYCE, 1992b). The principal, deviatoric components of the back stress tensor according to this eight-chain non-Gaussian network model are [cf. (31)]

$$B_i^{\text{8-ch}} = \frac{1}{3} C^{\mathrm{R}} \sqrt{N} \frac{\lambda_i^{\mathrm{p}2} - \lambda^{\mathrm{p}2}}{\lambda^{\mathrm{p}}} \mathscr{L}^{-1}\left(\frac{\lambda^{\mathrm{p}}}{\sqrt{N}}\right), \quad \lambda^{\mathrm{p}2} = \frac{1}{3} \sum_{j=1}^{3} \lambda_j^{\mathrm{p}2}. \tag{40}$$

On the basis of our considerations in the previous section for rubber-like materials, we can now also consider the full network model, in which full account is given of the orientation distribution of the individual chains in the network. According to this model, the principal back stresses are given by [cf. (29)]

$$B_i = \frac{1}{4\pi} C^{\mathrm{R}} \sqrt{N} \int_0^{\pi} \int_0^{2\pi} \mathscr{L}^{-1}\left(\frac{\lambda^{\mathrm{p}}}{\sqrt{N}}\right) \frac{\lambda_i^{\mathrm{p}2}(m_i^0)^2 - \frac{1}{3}\lambda^{\mathrm{p}2}}{\lambda^{\mathrm{p}}} \sin\theta_0 \, \mathrm{d}\theta_0 \, \mathrm{d}\varphi_0,$$

$$\lambda^{\mathrm{p}2} = \sum_i (m_i^0)^2 \lambda_i^{\mathrm{p}2}, \tag{41}$$

with m_i^0 defined by (21) and with λ^{p} being defined similar to (24). Here, the averaging is carried out in the initial configuration. Alternatively, B_i can be identified in the Eulerian form [cf. (28)]

$$B_i = \frac{1}{4\pi} C^{\mathrm{R}} \sqrt{N} \int_0^{\pi} \int_0^{2\pi} \mathscr{L}^{-1}\left(\frac{\lambda^{\mathrm{p}}}{\sqrt{N}}\right) \lambda^{\mathrm{p}4}(m_i^2 - \tfrac{1}{3}) \sin\theta \, \mathrm{d}\theta \, \mathrm{d}\varphi, \quad \lambda^{\mathrm{p}-2} = \sum_i m_i^2 / \lambda_i^{\mathrm{p}2}, \tag{42}$$

with m_i defined by (20) and with λ^p according to a similar expression to (25). Similar to (32) for rubber-like materials, an approximation of the full network predictions can be sought in the form of a combination of the three-chain and eight-chain models through

$$B_i = (1-\rho_p)B_i^{3\text{-ch}} + \rho_p B_i^{8\text{-ch}}, \tag{43}$$

thus avoiding the time-consuming integration involved in (41) and (42). Here, ρ_p is considered to be related to the maximal principal plastic stretch $\lambda^p_{max} = \max(\lambda^p_1, \lambda^p_2, \lambda^p_3)$ via $\rho_p = 0.85\lambda^p_{max}/\sqrt{N}$. Assuming that the actual physically entangled molecular chains behave sufficiently close to a perfect non-Gaussian network, this full network model should give a more accurate description than the approximate three- and eight-chain models. In this spirit, the full network model will now be used to assess the adequacy of the simplified hardening expressions (39) and (40).

3.3. *Results*

Arruda and Boyce (1992b) give a detailed discussion of the predictions of the above mentioned constitutive models using either the three-chain or the eight-chain network model in comparison with experimental results on PC and PMMA. In particular, they study the accuracy with which the orientational hardening in these materials can be predicted with these simplified models under different states of deformation, viz. uniaxial compression and plane strain compression. Here we wish to reconsider one of their series of tests in order to assess the deviation of these approximate network models based on expressions (39) and (40) from the more exact full network description contained in (41) and (42). These tests relate to uniaxial or plane strain compression of PC at room temperature ($T = 23^\circ$C), which are specified by the following velocity gradient components with respect to a global Cartesian basis:

uniaxial compression

$$[L_{ij}] = \begin{bmatrix} -\dot{\varepsilon} & 0 & 0 \\ 0 & \dot{\varepsilon}_\perp & 0 \\ 0 & 0 & \dot{\varepsilon}_\perp \end{bmatrix}$$

plane strain compression

$$[L_{ij}] = \begin{bmatrix} -\dot{\varepsilon} & 0 & 0 \\ 0 & \dot{\varepsilon}_\perp & 0 \\ 0 & 0 & 0 \end{bmatrix}.$$

The applied strain-rate was taken as $\dot{\varepsilon} = 0.01/s$, and the transverse strain-rate $\dot{\varepsilon}_\perp$ is determined from the boundary conditions $\sigma_{22} = \sigma_{33} = 0$ and $\sigma_{22} = 0$ for uniaxial and plane strain compression, respectively. The stress response in terms of the compressive stress $\sigma = -\sigma_{11}$ versus the logarithmic strain ε is obtained by numerically integrating the BPA constitutive equations (34)–(38) in an incremental manner. The back stresses are at each increment computed from the current plastic stretch; in the case of the full network model, we used the expressions (41) and applied the same numerical integration scheme as in Section 2.6.

The values of the elastic and viscoplastic material parameters to be used in the simulation are based on tensile experiments on PC (Boyce and Arruda, 1990). Following Arruda and Boyce (1992b), the parameters C^R and N that determine the orientational hardening are fitted for all three network models to the uniaxial

compression data. However, as opposed to ARRUDA and BOYCE (1992b), we have chosen to use the same value of C^R for all three models, for the reason that C^R governs the network hardening at small plastic strains, while at that stage there is no conceivable difference yet between the various network models (see also Section 2.6). With the parameters thus obtained, the plane strain compression response is simulated and compared with the experimental results shown in Fig. 10. It is seen that the uniaxial response is picked up very accurately with each of the models with the chosen value of N; but these values cannot be determined very accurately because the maximum plastic stretches attained before failure are still far off the limit stretch. The various predicted plane strain responses exhibit the same tendency as found in the foregoing for rubber elasticity in Fig. 9: the plane strain responses according to the three- and eight-chain models provide upper and lower bounds, respectively, to the full network predictions. The best agreement with experiments is obviously obtained in this case with the eight-chain model.

As a further assessment of the adequacy of these network models, we will now consider the deformation of PC (at room temperature) by simple shear. This is a significantly different deformation process than the tension or compression tests, and has not been studied in this context before. The problem analysed is that of homogeneous simple shear in the x_1–x_2 plane, as determined by the velocity gradient components $L_{12} = \dot{\gamma}$, $L_{ij} = 0$ otherwise, implying a plane strain condition in the x_3-direction. Using a special test setup, G'SELL and GOPEZ (1985) were able to produce this state of deformation in a relatively large part of their specimen with good accuracy. In accordance with their room temperature experiments on PC, we consider a shear rate $\dot{\gamma} = 3 \times 10^{-3}\,\mathrm{s}^{-1}$. The material constants are taken to be the same as in the above compression cases.

Figure 11 shows the shear stress σ_{12} as a function of the shear strain γ. Also shown are a number of experimental points taken from G'SELL and GOPEZ (1985). This data is obtained from the measured overall shear force on the specimen and the macroscopic shear strain, and is expected not to give a very accurate estimate of the actual stress state associated with pure simple shear because of the observed shear band propagation and end effects (work that considers these effects in detail is currently in progress). Focussing attention here to the post-yield behaviour, it is seen that the actual orientational hardening remains much less than that predicted by the BPA model for any of the network models. In agreement with the above findings, the eight-chain model predicts the lowest hardening, but beyond a shear strain of $\gamma \approx 1$ the limit stretching feature of the network theory becomes noticeable, while the actual response shows rather little hardening anyway.

The secondary normal stresses σ_{11} and σ_{22} during simple shear are mainly due to the development and subsequent rotation of the induced anisotropy. It is well-known that the prediction of these phenomena generally shows a rather strong dependence on the constitutive models—in particular the description of anisotropic hardening; for large strain metal plasticity, this has been studied in detail by e.g. VAN DER GIESSEN *et al.* (1992). Figure 12 now shows the predicted normal stress σ_{22} as a function of the shear strain γ according to the present constitutive model. In all cases, the normal stress is rather small up to $\gamma \approx 1$. For larger shears, the three-chain model predicts very large compressive stresses that are associated with the stretching of the network

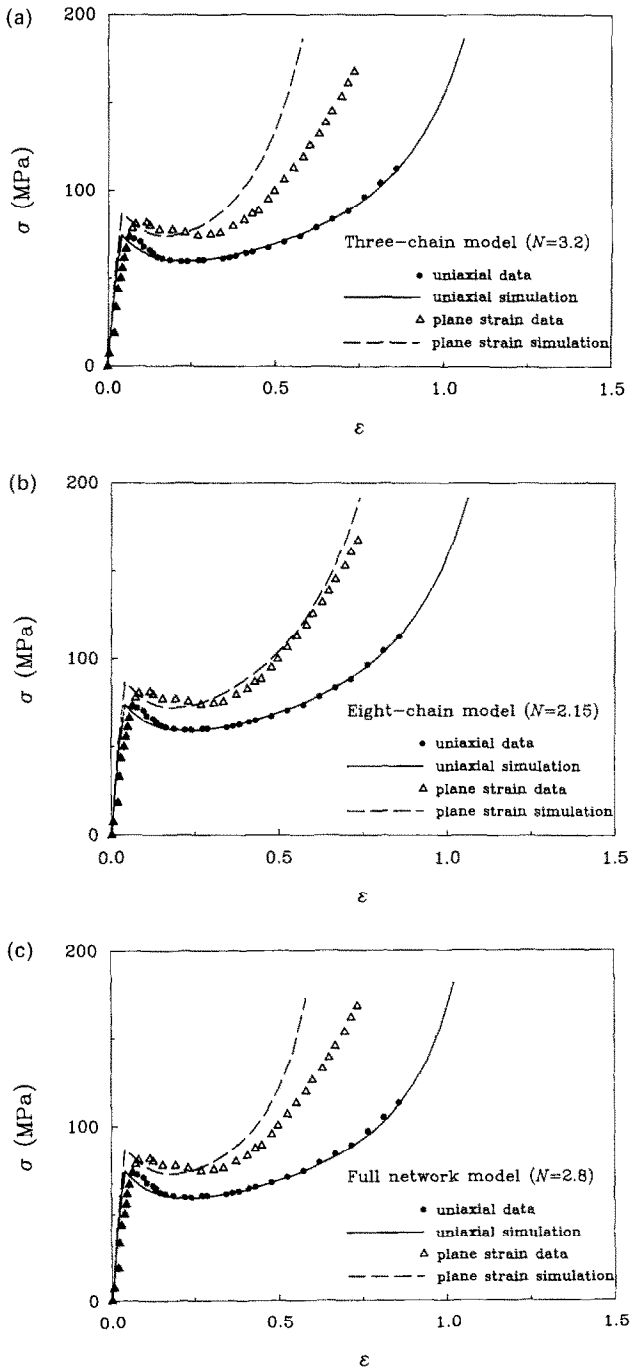

FIG. 10. Simulated true stress vs true strain curve for compression of PC at room temperature according to the three-chain (a), the eight-chain (b) and the full network model (c) for the orientation hardening. The experimental results are from ARRUDA and BOYCE (1992) and the material parameters used in the numerical simulation are $E = 2300$ MPa, $\nu = 0.3$, $\dot{\gamma}_0 = 2 \times 10^{15}$ s^{-1}, $A = 240$ K MPa^{-1}, $s_0 = 97$ MPa, $s_{ss}/s_0 = 0.79$, $h = 500$ MPa, $\alpha = 0.08$ and $C^R = 12.8$ MPa.

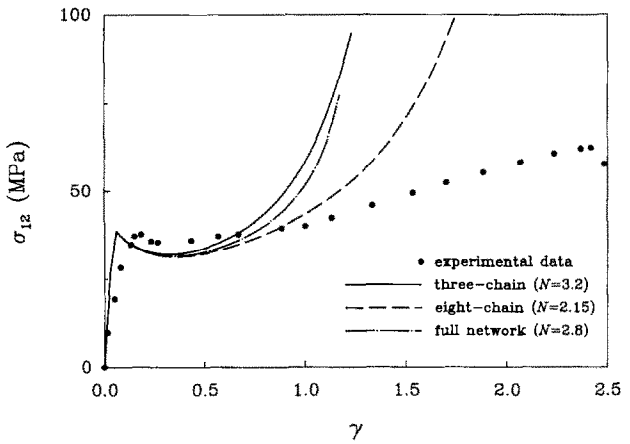

FIG. 11. Shear stress response to large simple shear of PC at room temperature at a shear strain-rate of $\dot{\gamma} = 3 \times 10^{-3}\,\mathrm{s}^{-1}$. The experimental data is estimated from the macroscopic load and shear strain data from G'SELL and GOPEZ (1985), and the material parameters used for the simulation are identical to those listed in Fig. 10.

affinely with the plastic deformation. Initially, the principal directions of the plastic stretch are oriented at roughly 45° relative to the x_1–x_2 axes, and this orientation slowly rotates towards the final ideal x_1–x_2 directions with ongoing shearing. The limit stretching of the network is attained long before such final orientations are reached, thus explaining the very substantial normal stress. The full network model predicts roughly the same normal stress development, but when using the eight-chain model, we see that the magnitude of the normal stress reduces drastically. Unfortunately, we have not been able to find any experimental data on normal stress

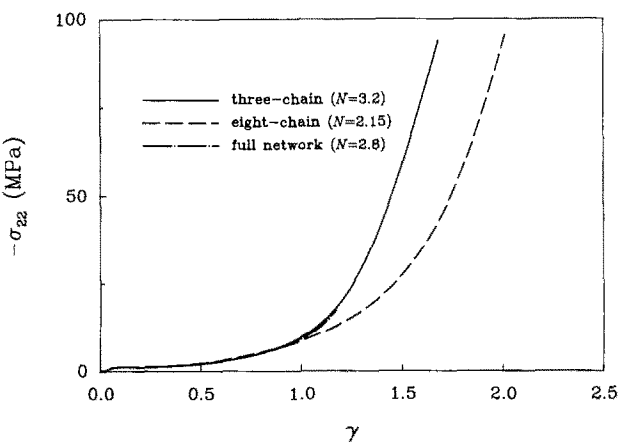

FIG. 12. Development of compressive normal stress during large simple shear of PC at room temperature. Strain-rate and material parameters are as in Fig. 11.

development during simple shear of PC in order to compare these predicted results with experiments. Nevertheless, it seems unlikely that the very large values for $\gamma > 1$ are realistic.

We have repeated the above mentioned analyses for PMMA using the material constants given by Boyce *et al.* (1988). The trends in shear stress and normal stress development were found to be qualitatively completely similar to the above results, and we shall therefore not discuss this further.

After this discussion of the accuracy of the various network representations, it is very pertinent to point out briefly that our predictions may be strongly dependent on a number of assumptions in the constitutive model. In particular one needs to realize that the idea of using an affine network theory to model the stretching of the molecular network assumes that the junction points in the network remain intact. However, it has been suggested in the literature (see e.g. Raha and Bowden, 1972; Botto *et al.*, 1987) that physical entanglements in amorphous polymers are being pulled out during deformation. In terms of our network model this would mean that the number of chains n reduces in the course of the deformation process, while the number of links N per chain increases, thus reducing the stiffness of the network. This aspect absolutely requires further study. Furthermore, there is the particular way of incorporating deformation-induced anisotropy by means of the effective stress concept in (36). This is probably rather important in the above simple shear considerations, where the stress history is nonproportional and significant rotations of the principal axes occur. A different approach may be found in e.g. Batterman and Bassani (1990).

4. Conclusion

We have carefully considered the so-called non-Gaussian affine network models for molecular networks, and their application to modelling rubber elasticity and the orientation hardening in glassy amorphous polymers. Our considerations have extended Treloar and Riding's (1979) analysis for uniaxial and biaxial extension of rubber networks to general three-dimensional deformation processes. Our full network model fully accounts for the spatial distribution of the orientation of the chain end-to-end vectors. The purpose of studying this model here in some detail is to assess the accuracy of two approximate models in which the network response is modelled by sampling a few particular chain orientations, namely the classical three-chain model first suggested by James and Guth (1943), and the eight-chain model proposed very recently by Arruda and Boyce (1991, 1992a).

The general tendency of the predictions of these simplified models compared with the more exact full network theory is that with the same network parameters, the three-chain model overestimates the stiffness of the network at large strains, while the eight-chain model underestimates the stiffness. At small strains the models are indistinguishable. Another important aspect is the capability of the different models to capture the dependence of the network response to the state of deformation. It turns out that the three-chain model is not capable of picking-up this dependence, whereas the eight-chain tends to overestimate the dependence of the state of deformation as compared with the full network model.

The predictions of the network models both for rubber elasticity and for orientation hardening in glassy polymers are compared with available experimental results. In studying the dependence of the state of deformation in rubber-like materials it was found that the full network gave a much better quantitative agreement with experiments than the classical three-chain model. On the other hand, the eight-chain model performed even better sometimes, although this is an approximation of the full network model. It thus seems that this performance is not an inherent feature of the eight-chain model; rather, this reminded us of the constitutive assumptions involved in the affine network theory. It has been noted that further improvement of this physically based model for rubber elasticity requires a better understanding of the role of various kinds of network defects in rubber-like materials that are not taken into account at present. The application to glassy polymers is based upon even stronger assumptions. We have also discussed that one of the most important phenomena that has been neglected in the present modelling is the pulling out of entanglements in such polymers. The present results employing the full network model indicate that this may give rise to a significantly softer response than expected on the basis of the perfect network model. However, most of these matters are not well understood yet, and are among the outstanding problems in polymer physics.

In addition to a complete description of the stress–strain response during network deformation, the present paper has contributed in a more general sense to the understanding of the evolution of molecular orientation in three dimensions during large deformations. General balance equations have been derived in both Eulerian and Lagrangian formulations, and together with the affine deformation assumption this has led to a description of molecular re-orientation in a continuous sense in terms of what we called the CODF. This CODF gives the volume fraction of the molecular chains in a certain orientation in space. The general solution has been derived in closed form for three-dimensional network distortions that are affine with the continuum, stretch. Apart from its key role in the development of the stress–strain relations, this solution may turn out to be useful for constitutive formulation of anisotropic behaviour connected with the orientation distribution of molecular chains.

Acknowledgements

We want to thank Mr G. Th. M. Stam for his assistance in preparing Fig. 4. Part of the work of EvdG was made possible by a fellowship of the Royal Netherlands Academy of Arts and Sciences.

References

ANAND, L. 1979 *J. appl. Mech.* **46,** 78.

ARGON, A. S. 1973 *Phil. Mag.* **28,** 839.

ARRUDA, E. M. and BOYCE, M. C. 1991 In *Anisotropy and Localization of Deformation* (edited by J.-P. BOEHLER and A. S. KHAN), p. 483. Elsevier Applied Science, London.

ARRUDA, E. M. and BOYCE, M. C. 1992a Submitted for publication.

Arruda, E. M. and Boyce, M. C.	1992b	Submitted for publication.
Ball, R. C., Doi, M., Edwards, S. F. and Warner, M.	1981	*Polymer* **22,** 1010.
Batterman, S. D. and Bassani, J. L.	1990	*Polym. Engng Sci.* **30,** 1281.
Botto, P. A., Duckett, R. A. and Ward, I. M.	1987	*Polymer* **28,** 257.
Boyce, M. C. and Arruda, E. M.	1990	*Polym. Engng Sci.* **30,** 1288.
Boyce, M. C., Parks, D. M. and Argon, A. S.	1988	*Mech. Mater.* **7,** 15.
Boyce, M. C., Parks, D. M. and Argon, A. S.	1989	*Int. J. Plasticity* **5,** 593.
Flory, P. J.	1944	*Chem. Rev.* **35,** 51.
Flory, P. J. and Rehner, J.	1943	*J. Chem. Phys.* **11,** 512.
Gao, J. and Weiner, J. H.	1991	*Macromolecules* **24,** 5179.
G'Sell, C. and Gopez, A. J.	1985	*J. Mater. Sci.* **20,** 3462.
Haward, R. N. and Thackray, G.	1968	*Proc. R. Soc. Lond.* **A302,** 453.
James, A. G., Green, A. and Simpson, G. M.	1975	*J. appl. Polymer Sci.* **19,** 2033.
James, H. M. and Guth, E.	1943	*J. Chem. Phys.* **11,** 455.
Kuhn, W. and Grün, F.	1942	*Kolloid Z.* **101,** 248.
Lee, E. H.	1969	*J. appl. Mech.* **36,** 1.
Mark, J. E. and Erman, B.	1988	*Rubberlike Elasticity: A Molecular Primer.* Wiley, New York.
Ogden, R. W.	1984	*Non-linear Elastic Deformations.* Ellis Horwood Ltd., Chichester.
Raha, S. and Bowden, P. B.	1972	*Polymer* **13,** 174.
Treloar, L. R. G.	1944	*Trans. Faraday Soc.* **40,** 59.
Treloar, L. R. G.	1946	*Trans. Faraday Soc.* **42,** 83.
Treloar, L. R. G.	1954	*Trans. Faraday Soc.* **50,** 881.
Treloar, L. R. G.	1975	*Physics of Rubber Elasticity* (3rd edn). Oxford Univ. Press, Oxford.
Treloar, L. R. G. and Riding, G.	1979	*Proc. R. Soc. Lond.* **A369,** 261.
Van der Giessen, E., Wu, P. D. and Neale, K. W.	1992	*Int. J. Plasticity* (in press).
Wang, M. C. and Guth, E. J.	1952	*J. Chem. Phys.* **20,** 1144.
Wu, P. D. and Van der Giessen, E.	1992	*Mech. Res. Comm.* **19,** 427.